REVIEW

Check for updates

Upgrading earth-abundant biomass into three-dimensional carbon materials for energy and environmental applications

Shaofeng Zhou,[a] Lihua Zhou,[b] Yaping Zhang,*[a] Jian Sun,[a] Junlin Wen[a] and Yong Yuan ID *[a]

The "trash to treasure" process has been extensively demonstrated for various energy and environmental issues in the past few decades. Abundant biomass is well accepted as a carbon-rich, sustainable, and renewable precursor, offering us a plethora of possibilities for advanced materials for energy conversion and storage as well as environmental treatments; spatial modification of biomass facilitates the formation of a unique three-dimensional (3D) structure with micro- to macropores, yielding higher surface area and enhanced physicochemical properties. This novel concept provides sufficient reaction sites, excellent adsorption capability, more activated sites for catalyst doping, and fascinating electrochemical performance. Basically, the 3D cadre of biomass-derived carbon strengthens the economic competitiveness of these materials and broadens their applications in fields such as in supercapacitors, chemical batteries, bioenergy harvest, adsorbents for organic pollutants and greenhouse gases, and efficient (photo)catalysts. The scope of this review mainly focuses on the most popular synthesis methodology of three-dimensional carbon materials derived from biomass and their critical applications in the fields of energy and environment.

1. Introduction

Global energy consumption and environmental burden have been rapidly increasing due to the significant increase in population, urbanization, and living standards in the last half century, and it is expected to keep increasing dramatically in the coming years.[1,2] The development of efficient, sustainable and clean energy sources and carriers, including bioenergy, lithium-ion batteries and supercapacitors, has become extremely urgent to satisfy the increasing demand of energy. Moreover, the quality of the environment has deteriorated due to industrialization and long-term agricultural activities; this has made it imperative to efficiently control and remove environmental contaminants.[3,4] In this context, improvement of the technology

[a]Guangzhou Key Laboratory Environmental Catalysis and Pollution Control, Guangdong Key Laboratory of Environmental Catalysis and Health Risk Control, School of Environmental Science and Engineering, Institute of Environmental Health and Pollution Control, Guangdong University of Technology, Guangzhou 510006, China. E-mail: yuanyong@soil.gd.cn; zhangyaping911@foxmail.com

[b]Institute of Natural Medicine & Green Chemistry, School of Chemical Engineering and Light Industry, Guangdong University of Technology, Guangzhou 510006, China
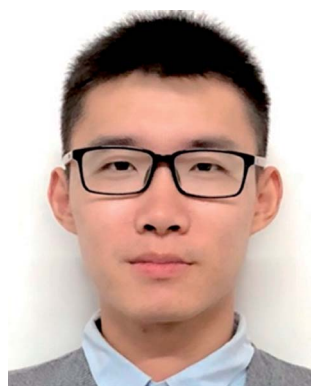
Shaofeng Zhou is currently a postdoctoral researcher in the School of Environmental Science and Technology at Guangdong University of Technology. He received his PhD in Environmental Science and Technology from South China University of Technology in 2018 and was a visiting PhD candidate in Technical University of Denmark from 2016 to 2017. He joined Prof. Yong Yuan's group in 2018. His research interest focuses on the development and use of microbial electrochemical systems toward environmental issues.

Lihua Zhou is a Professor of Chemistry at Guangdong University of Technology (GDUT). She obtained her PhD in Organic Chemistry in 2006 from Sun Yat-sen University, China. She joined School of Chemical Engineering and Light Industry at GDUT as a lecturer in 2006 and was promoted to Professor in 2018. She has authored over 20 articles in peer-reviewed journals. Her research focuses on the development of electrocatalysts and carbon materials for energy applications.

This journal is © The Royal Society of Chemistry 2019

J. Mater. Chem. A, 2019, **7**, 4217–4229 | 4217

and materials has shown significant promise for immense improvements.

In recent years, carbon materials have received significant research attention because of their potential applications in energy conversion, storage, and environmental monitoring as they have unique properties such as low capital cost, easy availability, nontoxicity, environmental friendliness, and biocompatibility. It has been widely considered that carbon-based materials play an important role in the effort to overcome major challenges in global energy consumption and environmental burden. In this regard, various carbon materials including activated carbon, carbon nanotubes, graphene, carbide-derived carbon, and templated carbon have been extensively explored. For example, significant efforts have been made towards the development of graphene-based materials for various kinds of Li batteries, supercapacitors, fuel cells, and water and air purification systems because of the unique structure, high surface area, and excellent chemical stability of graphene.[5–7] However, it has been found that defects such as poor dispersion, restacking, and multilayer fragility can prevent the complete realization of the physicochemical and high surface area properties of graphene.[8] Other carbon materials have also faced such similar drawbacks when used in energy devices and pollutant treatment techniques. To this end, it has become important to maintain the properties of carbon materials in bulk and to enhance graphite utilization for practical applications. One of the technical solutions is to construct solid three-dimensional (3D) networks of carbon, which could also be referred as hierarchical 3D structures, foams including templates, and aerogels.

3D carbon materials are the new hot topic in the fabrication of high-performance electrodes for renewable energy and environmental applications due to their structural interconnectivities, high electrical conductivity, and good mechanical stability.[9,10] Carbon materials with 3D configurations, including CNT-based networks, graphene-based architectures, polymer and metal–organic framework (MOF)-derived hierarchical porous carbons, and even more complex 3D carbon frameworks, have received considerable attention in the recent years.[10] These 3D carbon materials have shown promising potential for use in LIBs, supercapacitors, fuel cells, and environmental remediation techniques.[9,11–15] However, most of the abovementioned 3D carbon materials are costly due to the utilization of high-cost precursors, requirement of energy-intensive procedures, and involvement of unfriendly environmental practices. In this regard, the green synthesis of 3D carbon materials *via* cost-effective strategies is highly desirable.

Carbon-rich natural resources such as biomass and waste residues have the potential to serve as low cost, nontoxic, and renewable precursors for generating functional 3D carbon materials. During the past few years, many natural biomasses such as seaweed, moss, *Amaranthus*, Cattail, bamboo fungus, *Okara*, microorganisms, and bacterial cellulose,[16,17] have been reported as capable of being converted into functional 3D carbon materials. In this review, we aim to discuss some of the recent advances in the conversion of sustainable biomass precursors into various 3D carbon materials from resources and highlight their applications in environmental- and energy-related fields. Initially, we introduce the latest progress in controllably preparing 3D biomass-derived carbon materials (3D-BDC) with an understanding of the involved mechanisms. Then, the potential applications of the as-prepared 3D carbon materials in microbial fuel cells, LIBs, supercapacitors, electrocatalysts, and pollutant removal are discussed. Finally, we highlight the key challenges and predicted futuristic development trends in the fabrication of biomass-derived 3D carbon materials science (Fig. 1).

Yaping Zhang obtained his PhD in Environmental Engineering in 2014 from South China University of Technology, China. He joined School of Environmental Science and Technology at Guangdong University of Technology (GDUT) in 2014 and was promoted to Associate Professor in 2018. His research interests involve microbial electrochemistry and biotechnology development for wastewater treatment.

Yong Yuan is a Professor of Environmental Science and Technology at Guangdong University of Technology (GDUT). He obtained his PhD in Environmental Biotechnology in 2009 from Konkuk University, South Korea. He joined Guangdong Institute of Eco-environmental Science as an Assistant Professor in 2009 and was promoted to Professor in 2014. He joined School of Environmental Science and Technology at GDUT in 2017. He has authored over 100 articles in peer-reviewed journals and his current h-index is 28. His research interests involve microbial electrochemistry, microbial biotechnologies, and biomass-derived carbon materials for energy and environmental applications. Besides undertaking scientific endeavors, Yong is raising two lovely young boys.
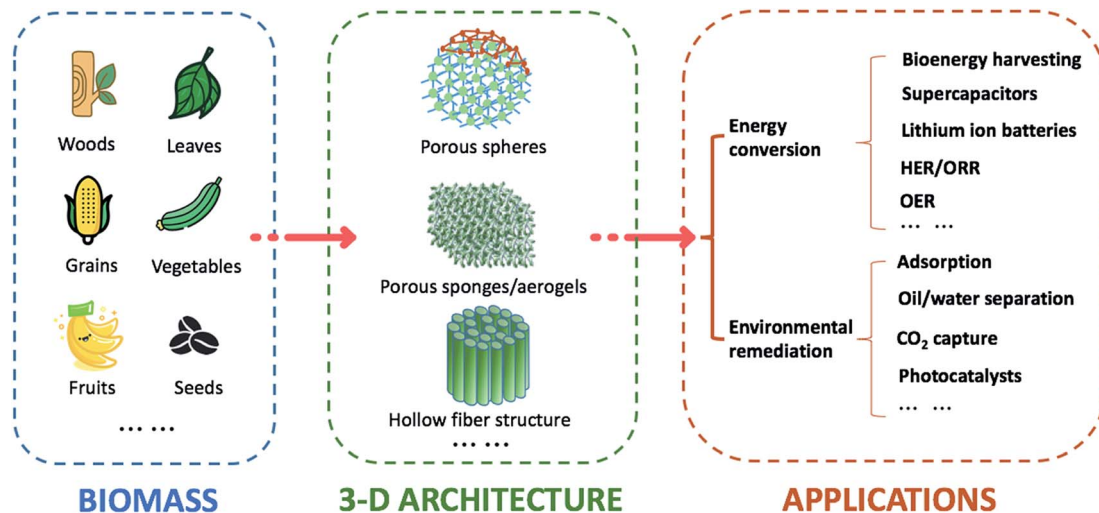
Fig. 1   Visual summary of the topical focus of this review. We have covered the recent developments in energy and environmental issues using biomass-derived 3D carbon materials.

2.   Fabrication of 3D carbon materials from biomass

Normally, general biomass, no matter where it originates from, should inevitably undergo a series of procedures before it can be turned into multifunctional 3D carbon materials; all the involved steps are dependent on other operating modifications. Several steps like thorough washing, freeze-drying, grinding into small pieces, sieving, and acidic treatments are inexorable pretreatments for further fabrications. In this section, we mainly outline the parts of the key processes or triggering techniques that are the most fashionable for fabricating 3D carbon materials with either exogenous or endogenous functional groups. Thermochemical conversion processes, like pyrolysis (including annealing, calcination), or hydrothermal syntheses to high carbon content are popularly used for carbonaceous materials. However, for some biomass carbon bulks, 3D architecture could not be obtained under a highly thermal condition. In this regard, a suitable heating process is imperative for 3D-BDC production.

2.1   Pyrolysis

Mostly, pyrolysis is a common strategy for raw carbon materials experiencing a typical heating process (200–1000 °C) in a noble gas or ammonia atmosphere, where the decomposition of organic biomass into either gaseous chemicals (*e.g.*, syngas) or solid carbon can occur. The residual products and their porosities/structures are tunable by controlling the elevating/end temperature and residence time.[18–20] In principle, the yield of the residual carbon contents is in a positive proportion to the end temperature and heating operation time, whereas the contents of the acid functional groups (*i.e.*, –COOH) have an opposite trend, resulting in higher hydrophobicity and graphitization.[21] Most importantly, pyrolysis (or so-called annealing) tends to be elaborately designed for the activation of certain catalyses. In particular, two-step pyrolysis was proposed for the synthesis of hierarchically porous 3D network nanocarbons derived from the organic biowaste of *Carassius auratus*.[22] In this case, pyrolysis with higher treating temperatures improved the contents of the endogenous graphitic-nitrogen doped on the nanocarbons, which was responsible for the enhanced oxygen reduction reaction (ORR). In addition, in a recent research, H. Li *et al.*[23] employed corncob and melamine as the carbon and nitrogen sources, respectively, to prepare a nano-tube@mesoporous carbon aerogel for use in electrochemical devices. The parameters in the pyrolysis procedure, the end temperature of which was set at 800 °C at a heating rate of 10 °C min^{-1} and 2 h residual time, were the key factors in the formation of the 3D architecture. In detail, a carbon-involved mixture was partially pyrolyzed to the gaseous portion that was subsequently catalyzed by using transition metals (iron, in this case) into N-doped CNTs in the presence of melamine. The internal iron element acted as the catalyst during pyrolysis. As a result, needle-like nanotubes were bountifully deposited onto the residual solid mesoporous structure. The 3D carbon composites eventually presented a specific capacitance of 538 F g^{-1} in aqueous electrolytes.[23] The formation of a morphological nexus highly relies upon the anthropogenic heating process and the selection of biomass resources. In this context, biomass-containing feasible cobalt, nickel, and iron are more favorable for catalyzing the interactions between carbon and hetero-atoms. Moreover, most biomasses themselves are resourceful in terms of heteroatomic elements such as N, P, and S; therefore, the heteroatom precursor is not inevitable in pyrolysis for heteroatom-doped 3D carbon supercapacitors.

Other than vegetative carbon precursors, bacterial cellulose from microbial growth is a type of special biomass and has received sufficient interest in the field of medical applications, wastewater treatments, and industrial utilization: the relevant details have been reviewed in earlier studies.[24,25] However, it is barely proposed as a common carbon precursor for 3D carbon

network evolutions. Typically, bacterial cellulose comprises on-site self-synthesized carbon-rich polymers formed *via* a series of complicated enzymatic cytoreactions by certain strains. At the same time, the bioconversion process—transforming low-molecular sugars into carbon hydrogels—slowly develops a 3D network on a template in the form of biomass. This procedure opens up a range of opportunities that functionalize so-called cellulose nanocrystals with other components (*e.g.*, rGO) to yield outstanding mechanical features, tailorable porosity, and high scalability with a marginal environmental impact because of its biocompatibility.[26] Bacterial cellulose as a carbon precursor, subsequently, undergoes thermal carbonization to yield 3D-BDC. Taking the model bacterial strain *A. xylinum* X-2 as an example, bacterial cellulose was grown layer-by-layer as a basic 3D matrix, followed by a series of fabrications with few-layer reduced graphene. The 3D nanocomposite possessed larger specific area and absorption capacities toward various oils and organic pollutants.[27] A recent study reported that bacterial cellulose from *A. xylinum* X-2 could be easily transferred into the 3D matrix through a milder method for fabricating fascinating electrodes for supercapacitors.[28] Although promising, difficulties such as time-consuming and complex multistep procedures surrounding the synthesis process remain fertile grounds for further optimization.

2.2 Hydrothermal synthesis

As compared to pyrolysis, hydrothermal carbonization is less energy-intensive as it is mainly operated at 100 °C to 300 °C wherein a 3D carbon structure can be achieved at low temperatures (below 250 °C).[21] Pretreated biomass dispersed in a liquid medium in a pressure-tight container (Teflon autoclave, for instance) would undergo one of the following (or combined) processes: hydrolysis, dehydration, decarboxylation, polymerization, and aromatization.[29] The hydrothermal method, in particular, firstly mildly hydrolyzes lignin and hemicellulose in biomass and continuously curves the porosity of biomass.[30] From this point of view, the contents of H and O in 3D carbon materials after hydrothermal treatment are normally higher than their counterparts after pyrolysis. For instance, Li *et al.* used rape pollen grains that were pretreated by a hydrothermal process to obtain macroscopic biochar with a reticulate structure.[31] It was the key step in the subsequent modification before they could become anode-building materials for Na-ion batteries.

2.3 Chemical activation

The activation of biomass carbon materials is an auxiliary but essential strategy that helps with materials' chemical state, inner 3D network nanostructure, high Brunauer–Emmett–Teller (BET) surface area, and porosity. Among a formidable range of activators, sodium/potassium hydroxide (KOH/NaOH), potassium chloride (KCl), potassium carbonate (K_2CO_3), zinc chloride ($ZnCl_2$), and phosphoric acid (H_3PO_4) are frequently mixed with biomass precursors for creating porous structures.[32] One basic mechanism is the caustic reaction in which the surface carbon of biomass could be consumed with activators at high temperatures, thereby introducing hierarchical porosity. Apart from these

common activators, carbon dioxide (CO_2) emerged as another activating agent usable for pore development.[33] One research reported polishment *via* CO_2 was responsible for hierarchical architecture in self-templated N-doped carbon material derived from bananas, and a 3D carbon material was achieved with high specific capacitance.[33] Under CO_2 thermal activation, the pores were first grown as micropores and then enlarged into macropores as the activation time increased.

2.4 Heteroatom doping

Heteroatoms are usually defined as a class of atoms that could replace carbon in the main molecular chain/ring, like the nitrogen in pyridazine. Common heteroatoms are nitrogen, oxygen, phosphorus, sulfur, halogens, and boron.[34] These heteroatoms are generally introduced *via* pyrolysis and hydrothermal synthesis under conditional operations to significantly enhance surface polarity, conductivity, and electron-donor tendency of materials, which is beneficial for a plethora of energy conversion devices.[18] Taking N-doped material as an example, its electrochemical properties of oxygen reduction are proposed to be comparable with Pt-related electrodes since nitrogen heteroatoms can significantly promote the bonding energy between the materials and O_2, reducing the overpotential of oxygen reduction.[34] For environmental issues, the high content of nitrogen yields powerful affinity *via* dipole–dipole interconnection, hydrogen bond, and electrostatic interaction with pollutants,[35] thereby making these materials promising for environmental remediation. Since the unique 3D construction of biomass-derived carbon lattice is capable of imparting sufficient reacting sites for heteroatoms doping, 3D carbon materials from biomass, which could functionalize maximum heteroatoms, have emerged into public consciousness. Recent efforts have been devoted toward using 3D-BDC materials for selective gas capture,[36] electrochemical catalysts,[37] establishment of ion batteries, and supercapacitors.[38] Moreover, numerous studies, among which ammonia chemicals (melamine, NH_3, NH_4^+, *etc.*) largely appeared for N-doping, have been conducted. For example, D. Li *et al.*[39] transferred *Gelidium amansii* into carbon nanofiber aerogel. Pyrolysis with NH_3 flow was subsequently carried out for doping nitrogen element, while the oxygen-containing groups in the biomass were partly converted into gaseous H_2O, CO, and CO_2. These results showed that the specific capacitance of N-doped 3D carbon was nearly five times higher than that of pristine carbon materials and presented excellent double-layer capacitive performance. In the meantime, most kinds of biomass themselves are nitrogen-rich; therefore, extrinsic nitrogen precursors become unnecessary.[40,41]

2.5 Other complementary approaches

Other than the aforementioned methods, there are several thermal–chemical extensions (*e.g.*, microwave carbonization) in which the reactants are heated on the molecular level by microwaves instead of traditional heating devices. The strongest merit of microwave carbonization is the tremendous reduction of operation time and, of course, improved energy

4220 | *J. Mater. Chem. A*, 2019, 7, 4217–4229

This journal is © The Royal Society of Chemistry 2019

efficiency. As compared to the hydrothermal method, the heating time could even be shortened to several minutes.[42] Deng *et al.* listed several assistive thermal–chemical systems in their review.[29] Taking molten salt synthesis (MSS) as an example, as its name implies, genera of inorganic salts like metal halides or oxide-involved salts for biomass-derived 3D carbon materials are introduced. In particular, low-melting-point salt (no more than 1000 °C) like zinc (potassium, sodium) chloride, carbonates, and nitrates are common salt agents employed in MSS by creating a liquid-flow phase for sufficient mass transfer and contact area at the solid–liquid interface.[43–45] Although the complete mechanism is still not understood, it is believed that molten salts can be used to fabricate valuable biomass-derived carbon materials with appropriate pore size distributions.[44] One report has suggested that in the MSS process, biomass annealed in air condition rather than inert gas atmosphere; this, to some extent, enhanced the electrochemical properties of the as-prepared porous carbon sheets for use in supercapacitors as oxygen took part in the introduction of porosity and forming pseudo-capacitance.[46] While MSS has been successfully applied in 3D-BDC preparation, salt agents and the ratio of carbon precursor and salt should be carefully selected because the end product of carbon and its properties are largely altered along with the different molten salt systems.

3. Applications

Due to the advantages of the 3D porous structure, as well as the worthwhile electrical, mechanical, and thermal properties of biomass-derived carbon, carbon materials exhibit outstanding electrochemical, catalytic, and chemical properties. They can be widely applied into energy generation and storage, catalyzing electrochemical reactions, and environmental remediation techniques. Here, we mainly summarize recent progresses in the applications of biomass-derived 3D carbon materials in these abovementioned fields.

3.1 Energy applications

3.1.1 Microbial energy harvesting. Microbial fuel cells (MFCs) are bioenergy-harvesting devices in which microorganisms in the anode convert chemical energy into electrical energy *via* a series of catalytic and enzymatic reactions. Because MFCs are capable of utilizing organic matter from various wastewaters to simultaneously generate electricity and treat wastewaters in an environmentally friendly manner, they have recently attracted extensive research attention.[47,48] It has been noticed that the performance of MFCs are dominated by electroactive bacteria that gather to form biofilms on the anode surface. Therefore, the anode materials of MFCs are the key components in determining power generation and wastewater treatment efficiency because they can act as harbors for biofilm formation as well as mediators for electron transfer.[49] Generally, anodes could perform better if anode materials have greater specific surface areas and higher affinity toward living microorganisms.[50] In this regard, 3D electrodes are good candidates for fabricating high-

performance MFCs because of their high active surface areas available for bacterial attachment. Numerous 3D electrodes, such as carbon scaffolds,[51] graphene/CNT sponges,[52] ceramics,[53] stainless steel foams,[54] and carbon brushes,[55] have been employed, and they have shown significant potential when used as anodes in MFCs. However, these 3D electrodes are usually costly and/or require complex procedures to synthesize. The direct conversion of low-cost natural macroporous materials *via* the pyrolysis of biomass provides an attractive way of producing low-cost high-performance 3D electrodes for MFCs. For example, Chen *et al.* and his co-workers separately converted kenaf[56] and pomelo peel[57] into 3D macroporous carbon electrodes, which showed good performance when used as anodes for microbial energy harvesting in MFCs. However, the pore sizes of the resulting 3D electrodes were in the range of micrometers, which resulted in pore clogging during long-term operations.[58] In this context, they fabricated 3D electrodes by pyrolyzing macroporous cardboard in which they observed that the thickness of the resulting 3D electrodes had a considerable impact on the performance.[58] It is noteworthy that current density of 390 A m^{-2} was achieved from a cardboard-derived 3D carbon electrode with 6 corrugated layers, which is the highest current density reported till date. Meanwhile, Yuan *et al.*[59] converted loofah sponge and polyaniline-modified loofah sponge into macroporous 3D carbon electrodes (LSC) and N-doped carbon-nanoparticle-modified 3D electrode (NCP/LSC), respectively, *via* pyrolysis (Fig. 2). The open 3D macrostructure facilitated biofilm growth, while the N-doped carbon nanoparticle effectively promoted extracellular electron transfer between the bacteria and the electrode. When employed as MFC anodes, NCP/LSC electrodes outperformed those of conventional 3D electrodes, such as unmodified LSC, graphite plate, carbon felt, commercially available reticulated vitreous carbon (RVC), and graphene-coated sponge electrodes. They reported that the LSC electrode could also be modified by TiO$_2$/carbon core–shell nanoparticles to improve the pseudocapacitance
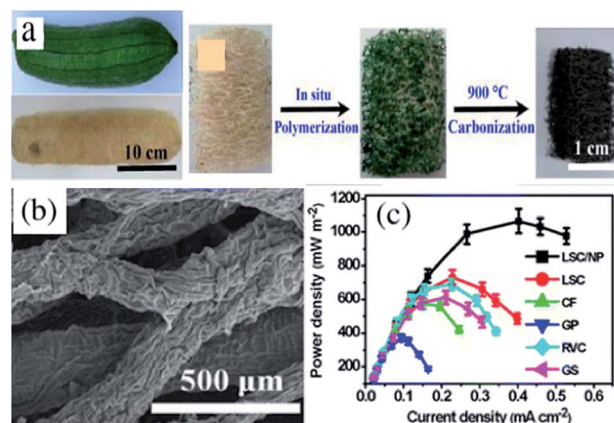

Fig. 2 (a) Images of the fresh loofah sponge and its carbonized materials; (b) SEM images of the as-prepared loofah sponge skeleton; (c) polarization curves of the MFC loofah sponge anode and different control anodes. Figures are reproduced with permission from ref. 59. Copyright 2013 American Chemical Society.

characteristics.[60] Detailed electrochemical analyses verified a positive correlation between the specific capacitance and MFC power density.[60] Moreover, other low-cost sustainable natural biomasses (*e.g.*, silk cocoon, mushroom, kapok, and chestnut) were also capable of being converted into high-performance 3D electrodes for microbial energy harvesting in MFCs.[61–64]

3.1.2 Supercapacitors. Supercapacitors, one of the most promising energy storage devices with high power density, highly reversible charge storage process, and long cycling life, have shown promising potential in applications such as hybrid vehicles, portable electronic devices, and other high-power applications.[65] Based on the energy storage mechanisms, supercapacitors can be divided into electrical double-layer capacitors (EDLCs), hybrid energy storage systems, and pseudocapacitors.[66] Porous carbon, particularly, activated carbon, is one of the most attractive materials for use in EDLCs due to its excellent electrochemical stability, high specific surface area, and abundant raw material.[67,68] However, the performance of porous-carbon-based supercapacitors is considerably limited by their low conductivity, high ion transport resistance, and insufficient ionic diffusion in the inner pores of porous carbon. Recent reports have indicated that 3D porous carbon materials with unique hierarchical porous structures have emerged as ideal candidates for high-performance supercapacitors.[69,70] As compared to conventional porous carbon materials, 3D porous carbon materials possess well-defined pore structures and topologies, providing minimized diffusive resistance to ion transport. 3D porous carbon materials are usually prepared from carbon sources of polymers with various templates and MOFs, which involve complicated and expensive processes. In this regard, natural biomasses have been considered as potential alternatives to polymer precursors because they are generally renewable, inexpensive, and environmentally benign.[71] Meanwhile, natural biomasses can be easily converted into carbon materials having 3D structural morphologies through both self-structuring and artificial regulation. For example, Zhang *et al.* developed porous carbon by using natural lignin as the precursor and KOH as the activating agent *via* a facile template-free method.[72] The obtained carbon material exhibited a 3D network with the distribution of macroporous cores, mesoporous channels, and micropores. The resulting 3D carbon material exhibited capacitance of 165.0 F g^{-1} in 1 M H$_2$SO$_4$ solution and excellent cycling stability after 5000 galvanostatic charge–discharge cycles. To further enhance the performance of supercapacitors, 3D carbon materials obtained from natural biomass were usually fabricated with metal oxides. For instance, Wu *et al.* have developed low-cost carbonaceous flexible hydrogels and aerogels by using watermelon as the carbon source *via* a facile, green, and template-free hydrothermal reaction.[73] The sponge-like carbonaceous gels had a 3D porous structure and exhibited high chemical activity and robust mechanical properties. After associating with Fe$_3$O$_4$, the resulting 3D Fe$_3$O$_4$/carbonaceous gel composites exhibited excellent capacitance of 333.1 F g^{-1} at a current density of 1 A g^{-1}.

The unique 3D porous structure of the composite facilitated the transportation of both electrolyte ions and electrons,

leading to high capacitance.[73] In this context, wood can open up a diverse range of possibilities for LIB electrodes because of its naturally patterned multichannel carbon framework.[74] Chen *et al.* have successfully developed an "all-wood-structured" asymmetric supercapacitor (ASC) in which activated wood carbon, wooden membrane, and MnO$_2$/wood carbon were employed as the anode, separator, and cathode, respectively.[75] The construction of ASC was ingeniously designed to fulfill the potential of wood-derived 3D carbon materials with promising merits such as low tortuosity, high ionic and electronic conductivities, and high structural stability regardless of electrode deformation, presenting high energy density (approximately 1.6 mW h cm^{-2} at 1044 mW cm^{-2}) and long cycling life.[75] Other carbon materials with 3D structures (*e.g.*, lotus pollen) have also been used as capacitors (Fig. 3).[76] The highest specific capacitances could even exceed 257 F g^{-1} and exhibit satisfying cycling stability after 2000 charge–discharge cycles, which is comparable to those from 3D carbon materials based on graphene and CNTs.[76] This indicates that natural carbon materials with renewable, low cost, and environmentally friendly properties would potentially replace the more conventional carbon materials for future capacitance development.

3.1.3 LIBs. Rechargeable LIBs were first introduced in 1991 and have been considered to be one of the most promising energy storage systems for portable electronic devices in the last 20 years.[77] Graphites with various morphologies and structures are important anode materials that have been widely used in commercial LIBs at present. However, graphite has a relatively low theoretical specific capacity of 372 mA h g^{-1}, limiting its future applications (*e.g.*, in electrical vehicles). In order to enhance the Li-ion storage capabilities of carbonaceous materials, endeavors have been devoted toward the exploration of porous amorphous carbon materials because pores can effectively improve the reversible Li$^+$-storage capacity and shorten
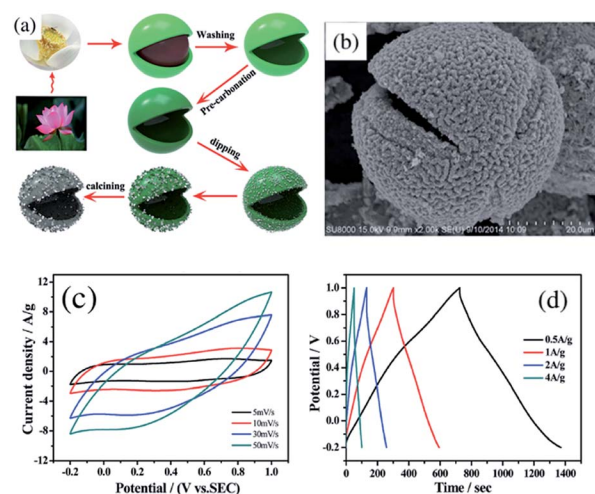

Fig. 3 (a) Schematic of the modification of 3D hollow MnO$_2$/carbon materials from lotus pollen grains; (b) SEM images of MnO$_2$/carbon materials; (c) CV and (d) galvanostatic charge–discharge curves at different scan rates. Figures are reproduced with permission from ref. 74. Copyright 2015 Royal Society of Chemistry.

4222 | *J. Mater. Chem. A*, 2019, **7**, 4217–4229

This journal is © The Royal Society of Chemistry 2019

the diffusion distances of Li^+. Recently, 3D porous carbon materials derived from CNTs, graphene, and synthesized polymers have also been tested for use as anode materials in LIBs.[10,78,79] The excellent Li^+-storage performance of such carbon materials can be attributed to their unique hierarchical porous structure that yields large active surfaces for adsorption, storage of Li ions, and fast paths for the transportation of Li ions. Meanwhile, 3D porous carbon materials obtained from natural biomass have exhibited promising potential as alternatives for the abovementioned carbon materials in LIBs.[80–82] For instance, 3D hierarchical porous carbon obtained from lignin was developed to serve as a promising LIB anode material, which enabled fast charge–discharge.[83] The LIB obtained from the resulting lignin-derived porous carbon anode displayed stable, high capacity of 470 mA h g^{-1} after 400 galvanostatic charge–discharge cycles at current density of 200 mA g^{-1}, which was significantly superior to commercial graphite anodes. Similarly, Chen *et al.* recently demonstrated a new concept in which natural basswood slices were upgraded into highly conductive, ultralight 3D carbon frameworks for current collection.[84] Such electrodes delivered attractive capacity of 7.6 mA h cm^{-2} at current density of 0.5 mA cm^{-2}.[84] Although wood biomass needs to be subjected to a two-step heating procedure to be fully carbonized, the as-prepared electrode exhibited striking mechanical strength and stability. This property could be attributed to the strong mechanical robustness of wood cellulose.[74] More information regarding wood-derived 3D materials has been comprehensively reviewed in recent studies.[74,85]

In addition, element-doped carbon electrodes for LIBs have been widely developed. For instance, N-doped carbon aerogels have been fabricated by extracting alginate from seaweed.[86] Their 3D morphology was revealed by SEM, and a large amount of interconnected macropores and large-sized mesopores were distinctly visible. The as-prepared aerogels had a high specific surface area of 2136 m^2 g^{-1} and reversible capacity of 550 mA h g^{-1} when used as the anode of LIBs.[86] Jiang *et al.*[87] also found that superior anode materials could be derived from bamboo chopsticks waste, where a simple and controllable hydrothermal (delignification) treatment and an associated carbonization process were used to convert used disposable bamboo chopsticks into uniform carbon fibers (Fig. 4). After growing nanostructured MnO_2 on the carbon fiber scaffold to form a 3D functionalized core–shell construction, LIBs with resulting composite anodes achieved high reversible capacity of 710 mA h g^{-1}, which was effectively maintained without decay up to 300 cycles.[87] It is noteworthy that 3D carbon materials derived from natural biomass can also exhibit promising performance as high-performance electrodes for Li–air, Li–S, and Na-ion batteries, due to their unique porous structures and worthwhile electrochemical properties.

3.1.4 Catalysts for oxygen reactions. Fabricating high-efficiency electrocatalysts for ORR and oxygen evolution reaction (OER) is of fundamental and economical importance for energy recovery technologies. An efficient catalyst for ORR or OER requires high efficiency of electron transference and low electrochemical kinetic barriers, thereby requiring precursors
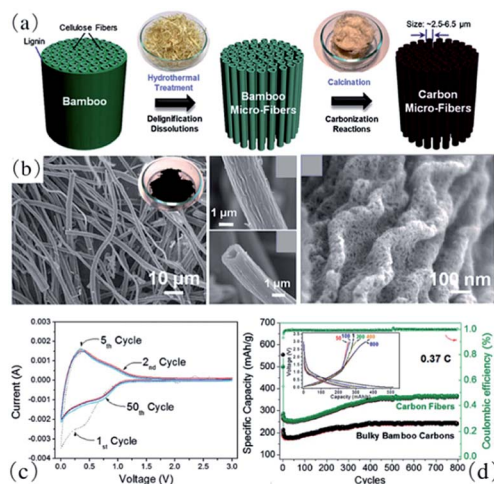

Fig. 4 (a) Schematic of the evolution of sustainable anodes of a Li-ion battery from bamboo chopsticks; (b) SEM profiles of the as-prepared anode; (c) CV curves of carbon anodes, and (d) long-term performance in typical charge–discharge process. Figures are reproduced with permission from ref. 83. Copyright 2014 Royal Society of Chemistry.

that are stable and earth-abundant. However, most of the traditional catalysts for energy conversion devices involve noble metals (*e.g.*, Pt), which deters large-scale applications due to their high cost and vulnerability. Till date, extensive efforts have been devoted toward exploring satisfying alternatives toward the aforementioned oxygen reactions, from transition metals assembly to nonmetallic porous architectures.[88,89] To this end, both ORR and OER catalysts with a 3D carbon structure derived from biomass have been increasingly favored and found to be lucrative as the building blocks for various practical fuel cells and metal–air battery constructions.[90–92] Recently, with different types of biomass as the carbon precursors, 3D metal-free catalysts have been reported in which the electrochemical oxygen reduction efficiencies of the heteroatom-doped catalysts are on par with those of commercial Pt/C catalysts.[93,94] In terms of robustness, a highly activated pH-universal ORR catalyst was synthesized from water lettuces as it exhibited impressive catalytic performance in alkaline, neutral, and acidic electrolytes of Zn–air alkaline fuel cells, methanol fuel cells, and MFCs, respectively,[37] indicating broad-spectrum practical applications. In addition, with the biomass cadre, non-precious-metal-involved catalysts were also developed into a 3D structure that significantly improved the size of the mesopores.[95] For instance, Liu *et al.* reported an effective strategy for the synthesis of 3D porous graphitic carbon nanoparticles ($Fe_2N@carbon$) by chelating iron with alginate isolated from seaweed. This carbonized material proved to be an excellent catalyst for four-electron reduction of oxygen.[96] Moreover, a recent study demonstrated that (heteroatom-doped) nanocarbon materials showed excellent ORR performance but poor OER ability. Therefore, a study was conducted in which pollen grains were decorated with transition metals (*i.e.*, Fe), which proved promising to the OER field in order to formulate bifunctional electrocatalysts (Fig. 5).[89] Generally, natural biomass materials have

put themselves on a considerable position for use in air-related energy devices because of their intrinsic merits such as scalability, activated electrochemical properties, and high specific surface areas. Nevertheless, despite ultralow cost, relevant financial computations and assessments have been rarely carried out or reported in recent articles, which should not be neglected from the perspective of practical applications.

3.1.5 Catalysts for hydrogen evolution reactions (HERs). Hydrogen gas is considered as the perfect next-generation energy source to replace fossil fuels since it is a clean and high-calorie energy carrier. Increasing pressures on calling for reliable technology has led to explosive growth in research toward highly efficient HER. Generally, most state-of-the-art technologies like steam–methane reformation and water electrolysis are typical endothermic reactions, limited by relatively low hydrogen evolution rate and high energy input.[97] In particular, steam–methane reformation, where hydrogen gas is upgraded from natural gas, suffers from undesirable byproducts like carbon dioxide/monoxide, reduced combustion heat, and increased separation cost.[98] On the other hand, water (photo)electrolysis could prove to be a sustainable approach as the only byproduct is oxygen gas, which could be employed into other value-added chemical synthesis processes. Although promising, low conversion rate from water to hydrogen gas (and/or oxygen gas) has been defined as the main bottleneck of HER's scalable applications and the corresponding electrodes (catalysts) are always immobilized with noble metals (e.g., Pt).[98] Therefore, there is still a long way to go for a quantum leap for ultralow-cost highly efficient robust cathode development for HER. Among the recent proposals, 3D biomass materials coupled with other noble-metal-free chemicals have been

reported as the ideal candidates for catalytic reactions of HER. Basically, the process for HER is partly an intuitive extension of ORR, where the catalysts transfer oxidizing equivalents (e.g., electrons) to water/H^+ and the priority behind such reaction is always lying in the improvement of the electro-driven conversion efficiency of the substrates.[99] To resolve this, a honeycomb-like multilayer N-rich carbon electrocatalyst was fabricated by Liu et al. from Bombyx mori silk cocoon.[99] The incredible catalytic performance and promising electrochemical durability for HER can be mainly attributed to the large amount of exposed active sites, high graphitization degree, and rich nitrogen elements (4.7%). Nitrogen element doping onto carbon materials is the key for facilitating hydrogen gas generation because of its metallic behavior, while a KCl activator facilitates the formation of a honeycomb-like porous surface with more exposed active sites. However, research involving earth-abundant biomass-derived 3D catalysts for HER is still in its infancy. Biomass is more often treated as feedstock for hydrogen generation rather than a catalyst. In this context, functional materials from nature should be continuously focused upon in studies.

3.2 3D biomass-derived materials for versatile environmental applications

3.2.1 Absorption of pollutants. The bright prospects of 3D-BDC materials are not only toward energy-related devices, but also in absorbents for the mitigation of environmental contaminants, including, but not limited to, heavy metal ions, organic wastes, and toxic agents.[100–103] When going through a brief history of absorbents, a kaleidoscope of biomass resources such as fruit peels,[104] silkworm cocoon,[105] lignocellulose fiber,[106] bacterial cellulose,[107] catkins,[108] cellulose,[109] cotton,[110] and bamboo[111] have emerged as ideal candidates for 3D-BDC preparation, and new materials are being appended to this list. Either way, the optimization of these materials toward achieving economic and practical competitiveness is predominantly benefitted from their innate merits of well-formed micro- to macrospores and outstanding property in solid–liquid interfaces for pollutants–solvents separation.[112,113] Generally, the spatial modification of materials in the form of film/thin cube,[113] foam,[114] sponge,[115] and carbon aerogel[116,117] facilitates improvements in specific surface area and lowering density of the materials, but also significantly improving the porous network, consequently enhancing the van der Waal's interactions or surface bond energies between the absorbents and pollutants.

Absorbents based on 3D-BDC are mainly known for their efficiency in water–oil separation. In particular, biomass with high cellulose content (e.g., sisal leaves) is more favored as an ideal precursor for carbon aerogel synthesis as cellulose is a key component when it comes to the materials' flexibility and mechanical strength (Fig. 6).[112] The hierarchical biomass-derived carbon-aerogel-deployed $SiO_2@MnO_2$ nanosheet exhibited high-level absorption capacity toward various oils (range: 60–120 g oil per g).[112] Another recent worthwhile research by Chen et al. critically depicted that corncob-lignin-
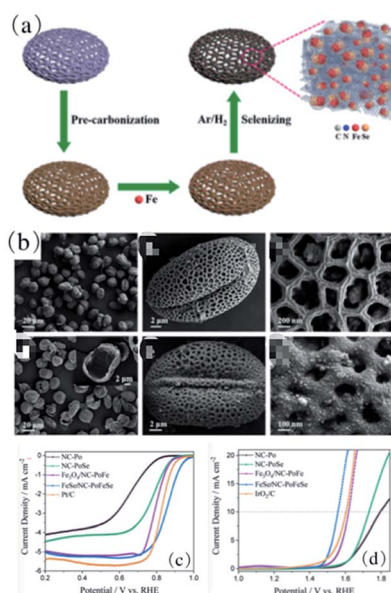

Fig. 5 (a) Schematic synthesis of bifunctional catalysts from pollen grains for the oxygen evolution and reduction reactions and (b) SEM profiles. The LSV curves of the as-prepared material and its counterparts for ORR (c) and OER (d), respectively. Figures are reproduced with permission from ref. 85. Copyright 2018 American Chemical Society.

modified graphene aerogels exhibited higher crude-oil-absorbing capability than its pristine counterpart.[118] Surface analyses indicated that this enhancement could be attributed to the high surface hydrophobicity and abundant 3D inter-connected porous architecture, which were observed as extreme incompact porous cadre, and consequently, yielding ultralow density. Meanwhile, the capacity of absorption toward oil could be optimized up to 522 times its own weight after carbonation treatment (800 °C in nitrogen atmosphere for 1 h).[118]

Other than aerogels, other forms of 3D-BDC such as foams, sponges, or other physical architectures have been popularly studied, too.[113,119,120] For instance, a mesoporous 3D wood membrane, in tandem with palladium nanoparticles, was implemented for methylene blue (MB)-containing artificial wastewater treatment.[113] The intensively arrayed but irregularly curved vessel channels internally grew in the wood and played an important role in the kinetics of the water flux, and it naturally acted as a perfect 3D skeleton and substrate for decorating Pd nanoparticles, which ultimately determined the MB removal efficiency (up to 99.8% at a treatment flow rate of 1×10^5 L (m^{-2} h^{-1})).

Till date, numerous studies have ceaselessly developed 3D-BDC porous absorbents because they potentially induce marginal side-effects and can be easily recycled and are biodegradable and cost-effective. These efforts not only facilitate the development of 3D-BDC absorbents, but also in various practical environmental remediation applications. Till now, frangibility—although many studies have presumed to have understood this phenomenon—is still the main challenge that limits future applications. Shortly, the various selections of biomass and synthesis approaches are no longer restraining factors for 3D-BDC evolution: attention should be carefully paid into the recoverability of pollutants and to definitely avoid the desorption of pollutants back into the environment, as well as the regenerability and longevity of absorbents in pollutant control applications.

3.2.2 CO$_2$ capture. 3D-BDC materials have been simultaneously used in greenhouse gas (CO$_2$) capture.[121] Tong *et al.* developed 3D N-self-doped carbons with hierarchical porous networks from chitosan. These carbons showed superior electrochemical properties, but also, importantly, achieved desirable CO$_2$ capture performance of 3.07–3.44 mmol g^{-1} (25 °C) due to the fact that the hierarchical framework mainly comprised nanorods and fiber-wall-interconnected porous carbons.[122] The intersectional architecture provided characteristic porosity for absorbing CO$_2$, and as stated in the studies, a porous structure can be further tailored for higher gas capture capacity.[122] Normally, mass transfer and gas diffusion rate of CO$_2$ are promising factors in a hierarchical carbon material because of its hybrid hollow distributions from micro- to meso(macro)porosity. Since there is a lack of specificity toward gas capture as it is more of a physical adsorption than a chemical process, these modified 3D-BDCs could be potentially applied into the absorption of various toxic gases (nitric oxide, *etc.*) and fine airborne particulate matter (PM2.5, *etc.*), thereby alleviating urban air pollution. Nevertheless, negligible relevant efforts have been reported.

3.2.3 Solar-assisted environmental remediation. Currently, there have been extensive efforts devoted toward the development of biomass-derived photosensitive catalysts.[123,124] Although bamboo has been proven to be a fine resource for generating photosensitive-dissolved mineral ash for reducing Cr(VI) in the presence of electron donors,[125] few reports have ever either emphasized the role of 3D architecture or the photoactivity of biomass derivatives themselves. Mostly, 3D-BDC was deployed as a basic but versatile skeleton for the synthesis of programmable photovoltaic composites to furnish as many integrating sites as possible for photo-semiconductor deposition. Shi *et al.* took winter melon as the biomass carbon resource, obtaining a sponge-like carbon aerogel through a hydrothermal process (Fig. 7).[126] TiO$_2$ nanoparticles were effectively anchored on the surface of the 3D architecture,
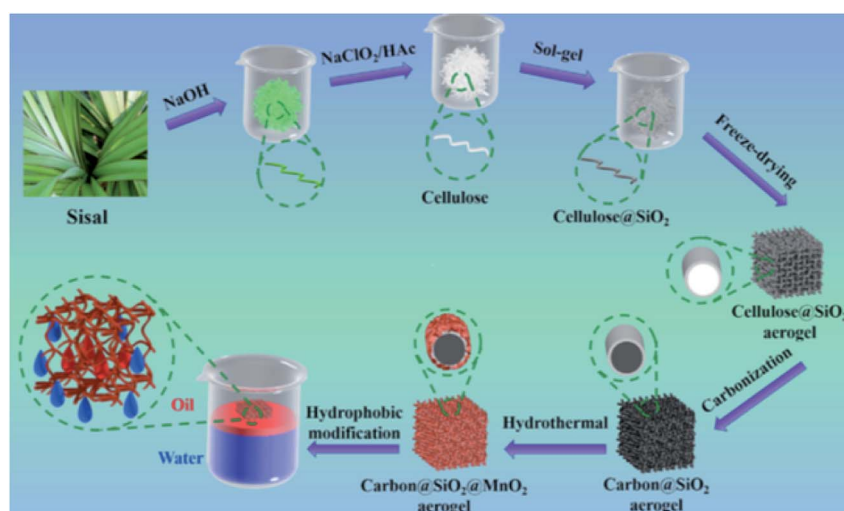

Fig. 6 Typical synthesis route for 3D carbon aerogels derived from sisal leaves for oil adsorption. Figure is reproduced with permission from ref. 108. Copyright 2018 Elsevier.

This journal is © The Royal Society of Chemistry 2019

J. Mater. Chem. A, 2019, **7**, 4217–4229 | **4225**

achieving higher efficiency of MB and ciprofloxacin photo-degradation than that of bare TiO_2.[126] Theoretically, a 3D structure was morphologically favored toward the immobilization of TiO_2 and other photosensitive semiconductors. It is believed that carbonized 3D biomass facilitates photoactivated electrons transport, thereby paving the way in suppressing the recombination of photoelectrons and hole pairs as a fine electron conductor.[127,128] In a recent report, Zhong and co-workers carbonized loofah and combined it with a typical semiconductor (SnS_2), forming a unique 3D functionalized biofoam.[128] This biofoam was able to reduce 99.7% $Cr(VI)$ within 2 h under visible-light illumination, while its counterpart without carbonization barely exhibited photocatalytic activity.[128] 3D carbonized biomass not only provides surface reaction sites *in vitro* for photocatalysts through its large specific area, but also, more importantly, integrates pollutant adsorption with photocatalytic degradation through its intricate channels and pores.

In addition, these perplexing channels and pores in biomass facilitated water transportation, which was used to fabricate solar steam generation devices. In this context, Chen *et al.* constructed a novel solar steam generation device for water purification by the layer-by-layer coating of black CNTs onto the *balsa* wood matrix.[129] The device merged the advantages of the photothermal properties of black CNTs and highly efficient water transpiration paths in natural channels of woods. Benefitting from this, the 3D device was able to recover 81% solar thermal energy at an evaporation rate of 11.22 kg m^{-2} h^{-1}.[129]
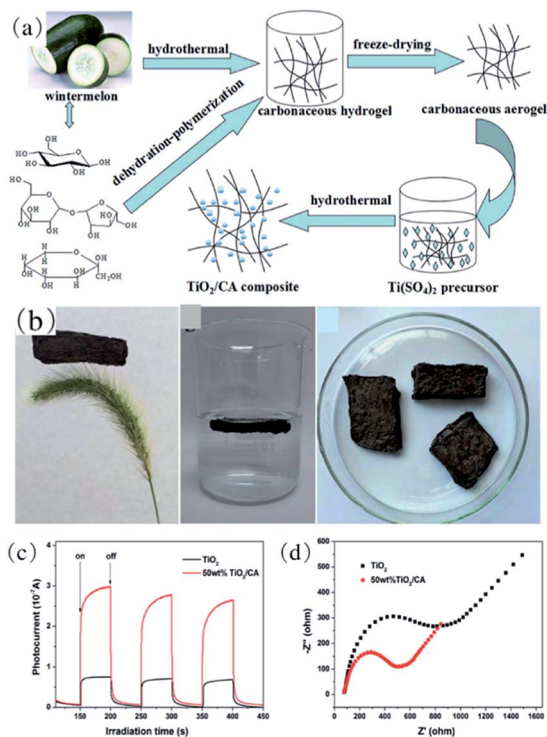

Fig. 7 (a) Procedure of 3D photocatalyst preparation from winter melon; (b) images of the ultralight materials; (c) photocurrent generation under illumination; and (d) EIS profiles of the catalyst. Figures are reproduced with permission from ref. 122. Copyright 2016 Royal Society of Chemistry.

4.   Conclusions and perspectives

Biomass is arguably one of the most abundant material on earth; therefore, biomass-derived carbon materials have become attractive solutions toward tackling green technology challenges of severe environmental issues and energy crises. The spatial modification to a 3D structure, normally, is partly a "trash to treasure" process that endows biomass with unexpected performance and bright prospective in relevant applications, turning biowaste into value-added chemicals. Promising studies have been conducted to explain the backbone of the synthesis mechanisms, environmental impact, and chemical electronics, and they are selectively elaborated in this review.

Nevertheless, some hurdles toward the upscaling of 3D-BDC should definitely be noted, as follows:

(1) Although there are diverse synthesis procedures available, the mechanical properties, as well as stability, of 3D-BDC should be paid close attention to as most fabrication approaches involve high-temperature carbonization. Although high temperature contributes toward the ultralightness and the conversion of micro- to macropores, thermal treatment (>800 °C) potentially leads to brittle 3D formations. This induces detrimental effects on the unique pore network of 3D-BDC, thereby deterring the scalability of such materials in either energy or environmental applications. Further material and structural engineering should be developed for tackling such issues.

(2) Thousands of studies on upgrading natural biomass are based on economic efficiency. However, it is difficult to find sufficient financial analysis in these articles. The capital cost is as important as the performance improvements, particularly for future commercialization and innovations of 3D-BDC. Lab-scale innovation is unfortunately far from sufficient. In addition, the lack of economical data creates continuing dilemma between technologies and markets, as well as causes a huge gap in the comparisons of different systems and synthesis methodologies. Sometimes, 3D-modified biomass with high performance suffers from poor durability and short lifetimes, which would, in turn, increase the operating cost.

(3) 3D-BDC could be applied as a versatile platform for carrying out research involving environmental issues, *e.g.*, acting as a natural carrier to investigate migration routes of heavy metals in polluted soil or used as sensitizers in the photochemical transportation of pollutants in aqueous solutions. Either way, redox reactions, physicochemical adsorption, and electrochemical catalysis are interfacial reactions, extensively involving electron transfer and mass transportation. Mechanisms behind the reactions remain a mystery. The construction of 3D-BDC will probably bring us new insights into micro-interfacial control in the transformation and removal of pollutants and provide fascinating tools to both qualitative and quantitative research.

(4) Normally, carbon derived from biomass experiences a series of natural aging processes including oxidation, acidification, and infection by bacteria, if it is employed in natural

4226 | *J. Mater. Chem. A*, 2019, **7**, 4217–4229

This journal is © The Royal Society of Chemistry 2019

environmental remediation. The aging process would more or less alter the elements and functional groups on the surface of carbon materials, resulting in alternative physicochemical properties. In this context, a process that mimics natural aging is liable to optimize performance. These "aged" materials always play a Janus influence, particularly in the reciprocal effects of biochar aging and heavy metal adsorption. Sometimes, they benefit from the fact that the specific surface area is increased. On the other hand, excessive aging sometimes destroys the performance; therefore, there are no criteria toward the optimal synthesis of a 3D carbon material from biomass. Hence, fundamental and mechanistic research and understanding is still necessitated.

Conflicts of interest

There are no conflicts to declare.

Acknowledgements

References

1 C. Li, T. Wang, B. Liu, M. Chen, A. Li, G. Zhang, M. Du, H. Wang, S. F. Liu and J. Gong, *Energy Environ. Sci.*, 2019, DOI: 10.1039/C8EE02768D.

2 M. Faraji, M. Yousefi, S. Yousefzadeh, M. Zirak, N. Naseri, T. H. Jeon, W. Choi and A. Z. Moshfegh, *Energy Environ. Sci.*, 2019, **12**, 59–95.

3 J. Radjenovic and D. L. Sedlak, *Environ. Sci. Technol.*, 2015, **49**, 11292–11302.

4 W. T. Mook, M. K. Aroua and G. Issabayeva, *Renewable Sustainable Energy Rev.*, 2014, **38**, 36–46.

5 A. Abbas, L. T. Mariana and A. N. Phan, *Carbon*, 2018, **140**, 77–99.

6 J. Ding, W. B. Hu, E. Paek and D. Mitlin, *Chem. Rev.*, 2018, **118**, 6457–6498.

7 A. J. Clancy, M. K. Bayazit, S. A. Hodge, N. T. Skipper, C. A. Howard and M. S. P. Shaffer, *Chem. Rev.*, 2018, **118**, 7363–7408.

8 D. Q. Li, B. W. Ren, Q. Y. Jin, H. Cui and C. X. Wang, *J. Mater. Chem. A*, 2018, **6**, 2176–2183.

9 B. Chen, Q. L. Ma, C. L. Tan, T. T. Lim, L. Huang and H. Zhang, *Small*, 2015, **11**, 3319–3336.

10 S. Dutta, A. Bhaumik and K. C. W. Wu, *Energy Environ. Sci.*, 2014, **7**, 3574–3592.

11 P. Y. Wang, B. J. Yang, G. H. Zhang, L. Zhang, H. Y. Jiao, J. T. Chen and X. B. Yan, *Chem. Eng. J.*, 2018, **353**, 453–459.

12 Z. Li, L. Zhang, X. Chen, B. Li, H. Wang and Q. Li, *Electrochim. Acta*, 2019, **296**, 8–17.

13 G. X. Lin, R. G. Ma, Y. Zhou, C. Hu, M. H. Yang, Q. Liu, S. Kaskel and J. C. Wang, *J. Colloid Interface Sci.*, 2018, **527**, 230–240.

14 Y. Song, T. Y. Liu, F. Qian, C. Zhu, B. Yao, E. Duoss, C. Spadaccini, M. Worsley and Y. Li, *J. Colloid Interface Sci.*, 2018, **509**, 529–545.

15 L. L. Bi, S. Q. Ci, P. W. Cai, H. Li and Z. H. Wen, *Appl. Surf. Sci.*, 2018, **427**, 10–16.

16 Z.-Y. Wu, H.-W. Liang, B.-C. Hu and S.-H. Yu, *Angew. Chem., Int. Ed. Engl.*, 2018, **57**, 15646–15662.

17 M. Yu, Y. Y. Han, Y. Li, J. Li and L. J. Wang, *Carbohydr. Polym.*, 2018, **199**, 555–562.

18 H. Huang, X. J. Wei and S. Y. Gao, *Electrochim. Acta*, 2016, **220**, 427–435.

19 J. Zhang, C. Y. Zhang, Y. F. Zhao, I. S. Amiinu, H. Zhou, X. B. Liu, Y. F. Tang and S. C. Mu, *Appl. Catal., B*, 2017, **211**, 148–156.

20 Y. J. Meng, T. M. Young, P. Z. Liu, C. I. Contescu, B. Huang and S. Q. Wang, *Cellulose*, 2015, **22**, 435–447.

21 Y. Yuan, N. Bolan, A. Prevoteau, M. Vithanage, J. K. Biswas, Y. S. Ok and H. L. Wang, *Bioresour. Technol.*, 2017, **246**, 271–281.

22 C. Z. Guo, R. Hu, W. L. Liao, Z. B. Li, L. T. Sun, D. P. Shi, Y. R. Li and C. G. Chen, *Electrochim. Acta*, 2017, **236**, 228–238.

23 H. X. Li, Y. Gong, C. P. Fu, H. H. Zhou, W. J. Yang, M. L. Guo, M. B. Li and Y. F. Kuang, *J. Mater. Chem. A*, 2017, **5**, 3875–3887.

24 M. Gullo, S. La China, P. M. Falcone and P. Giudici, *Appl. Microbiol. Biotechnol.*, 2018, **102**, 6885–6898.

25 N. Shah, M. Ul-Islam, W. A. Khattak and J. K. Park, *Carbohydr. Polym.*, 2013, **98**, 1585–1598.

26 Q. Jiang, D. Ghim, S. Cao, S. Tadepalli, K.-K. Liu, H. Kwon, J. Luan, Y. Min, Y.-S. Jun and S. Singamaneni, *Environ. Sci. Technol.*, 2019, **53**, 412–421.

27 H. L. Luo, J. Xie, J. Wang, F. L. Yao, Z. W. Yang and Y. Z. Wan, *Carbon*, 2018, **139**, 824–832.

28 H. L. Luo, J. J. Dong, Y. Zhang, G. Li, R. S. Guo, G. F. Zuo, M. D. Ye, Z. R. Wang, Z. W. Yang and Y. Z. Wan, *Chem. Eng. J.*, 2018, **334**, 1148–1158.

29 J. Deng, M. M. Li and Y. Wang, *Green Chem.*, 2016, **18**, 4824–4854.

30 M. Song, Y. Zhou, X. Ren, J. Wan, Y. Du, G. Wu and F. Ma, *J. Colloid Interface Sci.*, 2019, **535**, 276–286.

31 W. B. Li, J. F. Huang, L. L. Feng, L. Y. Cao, Y. J. Ren, R. Z. Li, Z. W. Xu, J. Y. Li and C. Y. Yao, *J. Alloys Compd.*, 2017, **716**, 210–219.

32 M. Gao, S. Y. Pan, W. C. Chen and P. C. Chiang, *Materials Today Energy*, 2018, **7**, 58–79.

33 E. Lei, W. Li, C. H. Ma, Z. Xu and S. X. Liu, *Appl. Surf. Sci.*, 2018, **457**, 477–486.

34 C. Z. Zhu, H. Li, S. F. Fu, D. Du and Y. H. Lin, *Chem. Soc. Rev.*, 2016, **45**, 517–531.

35 L. J. Lv, Y. Huang and D. P. Cao, *Appl. Surf. Sci.*, 2018, **456**, 184–194.

36 Y. Zhang, L. Liu, P. X. Zhang, J. Wang, M. Xu, Q. Deng, Z. L. Zeng and S. G. Deng, *Chem. Eng. J.*, 2019, **355**, 309–319.

This journal is © The Royal Society of Chemistry 2019

J. Mater. Chem. A, 2019, **7**, 4217–4229 | **4227**

37 L. Z. Liu, G. Zeng, J. X. Chen, L. L. Bi, L. M. Dai and Z. H. Wen, *Nano Energy*, 2018, **49**, 393–402.

38 S. X. Jiang, M. F. Chen, X. Y. Wang, Y. Zhang, C. Huang, Y. P. Zhang and Y. Wang, *Chem. Eng. J.*, 2019, **355**, 478–486.

39 D. H. Li, Y. Wang, Y. Y. Sun, Y. Lu, S. Chen, B. B. Wang, H. W. Zhang, Y. Z. Xia and D. J. Yang, *Carbon*, 2018, **137**, 31–40.

40 M. L. Wang, Y. Yao, Z. W. Tang, T. Zhao, F. Wu, Y. F. Yang and Q. F. Huang, *ACS Appl. Mater. Interfaces*, 2018, **10**, 32212–32219.

41 D. Y. Wu, Y. T. Shi, H. Y. Jing, X. Wang, X. D. Song, D. H. Si, S. X. Liang and C. Hao, *Int. J. Hydrogen Energy*, 2018, **43**, 19492–19499.

42 Y. F. Cheng, B. Q. Li, Y. J. Huang, Y. M. Wang, J. C. Chen, D. Q. Wei, Y. J. Feng, D. C. Jia and Y. Zhou, *Appl. Surf. Sci.*, 2018, **439**, 712–723.

43 Y. M. Chen, S. Ji, H. Wang, V. Linkov and R. F. Wang, *Int. J. Hydrogen Energy*, 2018, **43**, 5124–5132.

44 F. Yang, L. L. Sun, W. L. Xie, Q. Jiang, Y. Gao, W. Zhang and Y. Zhang, *Sci. Total Environ.*, 2017, **607**, 1391–1399.

45 H. S. Shang, Y. J. Lu, F. Zhao, C. Chao, B. Zhang and H. S. Zhang, *RSC Adv.*, 2015, **5**, 75728–75734.

46 C. J. Wang, D. P. Wu, H. J. Wang, Z. Y. Gao, F. Xu and K. Jiang, *J. Mater. Chem. A*, 2018, **6**, 1244–1254.

47 V. G. Gude, *J. Cleaner Prod.*, 2016, **122**, 287–307.

48 B. E. Logan, B. Hamelers, R. A. Rozendal, U. Schrorder, J. Keller, S. Freguia, P. Aelterman, W. Verstraete and K. Rabaey, *Environ. Sci. Technol.*, 2006, **40**, 5181–5192.

49 C. Santoro, C. Arbizzani, B. Erable and I. Ieropoulos, *J. Power Sources*, 2017, **356**, 225–244.

50 Y. Z. Zhang, L. F. Liu, B. Van der Bruggen and F. L. Yang, *J. Mater. Chem. A*, 2017, **5**, 12673–12698.

51 M. S. Jeon, Y. Jeon, J. H. Hwang, C. S. Heu, S. Jin, J. Shin, Y. Song, S. C. Kim, B. K. Cho, J. K. Lee and D. R. Kim, *Carbon*, 2018, **130**, 814–821.

52 H. T. Xu, J. S. Wu, L. J. Qi, Y. Chen, Q. Wen, T. G. Duan and Y. Y. Wang, *J. Appl. Electrochem.*, 2018, **48**, 1285–1295.

53 J. Winfield, I. Gajda, J. Greenman and I. Ieropoulos, *Bioresour. Technol.*, 2016, **215**, 296–303.

54 G. M. Wu, H. Bao, Z. Xia, B. Yang, L. C. Lei, Z. J. Li and C. X. Liu, *J. Power Sources*, 2018, **384**, 86–92.

55 S. F. Zhou, S. B. Huang, Y. Li, N. N. Zhao, H. Li, I. Angelidaki and Y. F. Zhang, *Talanta*, 2018, **186**, 368–371.

56 S. L. Chen, G. H. He, X. W. Hu, M. Y. Xie, S. Q. Wang, D. J. Zeng, H. Q. Hou and U. Schroder, *ChemSusChem*, 2012, **5**, 1059–1063.

57 S. L. Chen, Q. Liu, G. H. He, Y. Zhou, M. Hanif, X. W. Peng, S. Q. Wang and H. Q. Hou, *J. Mater. Chem.*, 2012, **22**, 18609–18613.

58 S. L. Chen, G. H. He, Q. Liu, F. Harnisch, Y. Zhou, Y. Chen, M. Hanif, S. Q. Wang, X. W. Peng, H. Q. Hou and U. Schroder, *Energy Environ. Sci.*, 2012, **5**, 9769–9772.

59 Y. Yuan, S. G. Zhou, Y. Liu and J. H. Tang, *Environ. Sci. Technol.*, 2013, **47**, 14525–14532.

60 J. H. Tang, Y. Yuan, T. Liu and S. G. Zhou, *J. Power Sources*, 2015, **274**, 170–176.

61 S. S. Chen, J. H. Tang, X. Y. Jing, Y. Liu, Y. Yuan and S. G. Zhou, *Electrochim. Acta*, 2016, **212**, 883–889.

62 R. Karthikeyan, B. Wang, J. Xuan, J. W. C. Wong, P. K. H. Lee and M. K. H. Leung, *Electrochim. Acta*, 2015, **157**, 314–323.

63 M. Lu, Y. J. Qian, C. C. Yang, X. Huang, H. Li, X. J. Xie, L. Huang and W. Huang, *Nano Energy*, 2017, **32**, 382–388.

64 H. L. Zhu, H. M. Wang, Y. Y. Li, W. Z. Bao, Z. Q. Fang, C. Preston, O. Vaaland, Z. Y. Ren and L. B. Hu, *Nano Energy*, 2014, **10**, 268–276.

65 W. Raza, F. Z. Ali, N. Raza, Y. W. Luo, K. H. Kim, J. H. Yang, S. Kumar, A. Mehmood and E. E. Kwon, *Nano Energy*, 2018, **52**, 441–473.

66 E. Lim, C. Jo and J. Lee, *Nanoscale*, 2016, **8**, 7827–7833.

67 N. Parveen, A. I. Al-Jaafari and J. I. Han, *Electrochim. Acta*, 2019, **293**, 84–96.

68 A. Dobashi, J. Maruyama, Y. H. Shen, M. Nandi and H. Uyama, *Carbohydr. Polym.*, 2018, **200**, 381–390.

69 M. Yu, Y. Y. Han, J. Li and L. J. Wang, *J. Porous Mater.*, 2018, **25**, 1679–1689.

70 L. Fang, Y. P. Xie, Y. Y. Wang, Z. W. Zhang, P. F. Liu, N. A. Cheng, J. F. Liu, Y. C. Tu, H. B. Zhao and J. J. Zhang, *Appl. Surf. Sci.*, 2019, **464**, 479–487.

71 Y. P. Gao, Z. B. Zhai, K. J. Huang and Y. Y. Zhang, *New J. Chem.*, 2017, **41**, 11456–11470.

72 W. L. Zhang, H. B. Lin, Z. Q. Lin, J. Yin, H. Y. Lu, D. C. Liu and M. Z. Zhao, *ChemSusChem*, 2015, **8**, 2114–2122.

73 X. L. Wu, T. Wen, H. L. Guo, S. B. Yang, X. K. Wang and A. W. Xu, *ACS Nano*, 2013, **7**, 3589–3597.

74 C. J. Chen and L. B. Hu, *Acc. Chem. Res.*, 2018, **51**, 3154–3165.

75 C. J. Chen, Y. Zhang, Y. J. Li, J. Q. Dai, J. W. Song, Y. G. Yao, Y. H. Gong, I. Kierzewski, J. Xie and L. B. Hu, *Energy Environ. Sci.*, 2017, **10**, 538–545.

76 H. P. Li, B. Wang, X. Y. He, J. Xiao, H. S. Zhang, Q. Liu, J. Y. Liu, J. Wang, L. H. Liu and P. Wang, *J. Mater. Chem. A*, 2015, **3**, 9754–9762.

77 Z. H. Chen, R. Amine, Z. F. Ma and K. Amine, *J. Phys. D: Appl. Phys.*, 2017, **50**, 14.

78 Y. M. Fan, W. L. Song, X. G. Li and L. Z. Fan, *Carbon*, 2017, **111**, 658–666.

79 Z. W. Zhang, Z. Q. Li, F. B. Hao, X. K. Wang, Q. Li, Y. X. Qi, R. H. Fan and L. W. Yin, *Adv. Funct. Mater.*, 2014, **24**, 2500–2509.

80 J. Zhang, J. Y. Xiang, Z. M. Dong, Y. Liu, Y. S. Wu, C. M. Xu and G. H. Du, *Electrochim. Acta*, 2014, **116**, 146–151.

81 Q. Jiang, Z. H. Zhang, S. Y. Yin, Z. P. Guo, S. Q. Wang and C. Q. Feng, *Appl. Surf. Sci.*, 2016, **379**, 73–82.

82 J. F. Wu, L. Zuo, Y. H. Song, Y. Q. Chen, R. H. Zhou, S. H. Chen and L. Wang, *J. Alloys Compd.*, 2016, **656**, 745–752.

83 W. L. Zhang, J. Yin, Z. Q. Lin, H. B. Lin, H. Y. Lu, Y. Wang and W. M. Huang, *Electrochim. Acta*, 2015, **176**, 1136–1142.

84 C. J. Chen, Y. Zhang, Y. J. Li, Y. D. Kuang, J. W. Song, W. Luo, Y. B. Wang, Y. G. Yao, G. Pastel, J. Xie and L. B. Hu, *Adv. Energy Mater.*, 2017, **7**, 8.

This journal is © The Royal Society of Chemistry 2019

85   H. L. Zhu, W. Luo, P. N. Ciesielski, Z. Q. Fang, J. Y. Zhu, G. Henriksson, M. E. Himmel and L. B. Hu, *Chem. Rev.*, 2016, **116**, 9305–9374.

86   J. L. Zhang, L. J. Zhang, S. L. Yang, D. H. Li, Z. X. Xie, B. B. Wang, Y. Z. Xia and F. Y. Quan, *J. Alloys Compd.*, 2017, **701**, 256–261.

87   J. Jiang, J. H. Zhu, W. Ai, Z. X. Fan, X. N. Shen, C. J. Zou, J. P. Liu, H. Zhang and T. Yu, *Energy Environ. Sci.*, 2014, **7**, 2670–2679.

88   P. Chen, L. K. Wang, G. Wang, M. R. Gao, J. Ge, W. J. Yuan, Y. H. Shen, A. J. Xie and S. H. Yu, *Energy Environ. Sci.*, 2014, **7**, 4095–4103.

89   N. Ma, Y. Jia, X. F. Yang, X. L. She, L. Z. Zhang, Z. Peng, X. D. Yao and D. J. Yang, *J. Mater. Chem. A*, 2016, **4**, 6376–6384.

90   H. Wu, J. Geng, H. T. Ge, Z. Y. Guo, Y. G. Wang and G. F. Zheng, *Adv. Energy Mater.*, 2016, **6**, 8.

91   F. L. Meng, L. Li, Z. Wu, H. X. Zhong, J. C. Li and J. M. Yan, *Chin. J. Catal.*, 2014, **35**, 877–883.

92   S. Y. Gao, H. Y. Liu, K. R. Geng and X. J. Wei, *Nano Energy*, 2015, **12**, 785–793.

93   H. W. Liang, Z. Y. Wu, L. F. Chen, C. Li and S. H. Yu, *Nano Energy*, 2015, **11**, 366–376.

94   Y. N. Yu, M. Q. Wang and S. J. Bao, *J. Solid State Electrochem.*, 2017, **21**, 103–110.

95   D. H. Li, C. X. Lv, L. Liu, Y. Z. Xia, X. L. She, S. J. Guo and D. J. Yang, *ACS Cent. Sci.*, 2015, **1**, 261–269.

96   L. Liu, X. F. Yang, N. Ma, H. T. Liu, Y. Z. Xia, C. M. Chen, D. J. Yang and X. D. Yao, *Small*, 2016, **12**, 1295–1301.

97   A. Speltini, A. Scalabrini, F. Maraschi, M. Sturini, A. Pisanu, L. Malavasi and A. Profumo, *Int. J. Hydrogen Energy*, 2018, **43**, 14925–14933.

98   R. Chaubey, S. Sahu, O. O. James and S. Maity, *Renewable Sustainable Energy Rev.*, 2013, **23**, 443–462.

99   X. R. Liu, M. Zhang, D. N. Yu, T. Li, M. Wan, H. Zhu, M. L. Du and J. M. Yao, *Electrochim. Acta*, 2016, **215**, 223–230.

100 J. H. Zhu, Q. Liu, Z. S. Li, J. Y. Liu, H. S. Zhang, R. M. Li, J. Wang and G. A. Emelchenko, *Dalton Trans.*, 2017, **46**, 420–429.

101 N. Mahfoudhi and S. Boufi, *Cellulose*, 2017, **24**, 1171–1197.

102 H. Zhang, Y. Q. Li, R. H. Shi, L. H. Chen and M. Z. Fan, *Carbohydr. Polym.*, 2018, **200**, 611–615.

103 L. Liu, J. P. Xie, Y. J. Li, Q. Zhang and J. M. Yao, *Cellulose*, 2016, **23**, 723–736.

104 X. J. Yue, T. Zhang, D. Y. Yang, F. X. Qiu and Z. D. Li, *J. Cleaner Prod.*, 2018, **199**, 411–419.

105 J. T. Sun, Z. P. Zhang, J. Ji, M. L. Dou and F. Wang, *Appl. Surf. Sci.*, 2017, **405**, 372–379.

106 N. Lavoine and L. Bergstrom, *J. Mater. Chem. A*, 2017, **5**, 13.

107 Y. Z. Wan, F. S. Zhang, C. Z. Li, G. Y. Xiong, Y. Zhu and H. L. Luo, *J. Mater. Chem. A*, 2015, **3**, 24389–24396.

108 L. L. Zang, Z. P. Bu, L. G. Sun and Y. H. Zhang, *RSC Adv.*, 2016, **6**, 48715–48719.

109 A. W. Carpenter, C. F. de Lannoy and M. R. Wiesner, *Environ. Sci. Technol.*, 2015, **49**, 5277–5287.

110 R. J. Lin, A. Li, T. T. Zheng, L. B. Lu and Y. Cao, *RSC Adv.*, 2015, **5**, 82027–82033.

111 H. Zhang, Y. Q. Li, Y. G. Xu, Z. X. Lu, L. H. Chen, L. L. Huang and M. Z. Fan, *Phys. Chem. Chem. Phys.*, 2016, **18**, 28297–28306.

112 D. S. Yuan, T. Zhang, Q. Guo, F. X. Qiu, D. Y. Yang and Z. P. Ou, *Chem. Eng. J.*, 2018, **351**, 622–630.

113 F. J. Chen, A. S. Gong, M. W. Zhu, G. Chen, S. D. Lacey, F. Jiang, Y. F. Li, Y. B. Wang, J. Q. Dai, Y. G. Yao, J. W. Song, B. Y. Liu, K. Fu, S. Das and L. B. Hu, *ACS Nano*, 2017, **11**, 4275–4282.

114 O. Oribayo, X. S. Feng, G. L. Rempel and Q. M. Pan, *Chem. Eng. J.*, 2017, **323**, 191–202.

115 Z. Zhang, G. Sebe, D. Rentsch, T. Zimmermann and P. Tingaut, *Chem. Mater.*, 2014, **26**, 2659–2668.

116 Y. G. Wang, S. Yadav, T. Heinlein, V. Konjik, H. Breitzke, G. Buntkowsky, J. J. Schneider and K. Zhang, *RSC Adv.*, 2014, **4**, 21553–21558.

117 Y. Xiong, C. Wang, H. W. Wang, Q. F. Yao, B. T. Fan, Y. P. Chen, Q. F. Sun, C. D. Jin and X. J. Xu, *J. Mater. Chem. A*, 2017, **5**, 5813–5819.

118 C. Z. Chen, F. F. Li, Y. R. Zhang, B. X. Wang, Y. M. Fan, X. L. Wang and R. C. Sun, *Chem. Eng. J.*, 2018, **350**, 173–180.

119 S. Wang, X. W. Peng, L. X. Zhong, J. W. Tan, S. S. Jing, X. F. Cao, W. Chen, C. F. Liu and R. C. Sun, *J. Mater. Chem. A*, 2015, **3**, 8772–8781.

120 J. Rong, F. X. Qiu, T. Zhang, X. Y. Zhang, Y. Zhu, J. C. Xu, D. Y. Yang and Y. T. Dai, *Chem. Eng. J.*, 2017, **322**, 397–407.

121 K. M. Nelson, S. M. Mahurin, R. T. Mayes, B. Williamson, C. M. Teague, A. J. Binder, L. Baggetto, G. M. Veith and S. Dai, *Microporous Mesoporous Mater.*, 2016, **222**, 94–103.

122 X. Tong, H. Zhuo, S. Wang, L. X. Zhong, Y. J. Hu, X. W. Peng, W. J. Zhou and R. C. Sun, *RSC Adv.*, 2016, **6**, 34261–34270.

123 Y. L. Wang, T. Song, P. Y. Zhang, T. B. Huang, T. Wang, T. T. Wang and H. P. Zeng, *ACS Sustainable Chem. Eng.*, 2018, **6**, 11536–11546.

124 P. Lisowski, J. C. Colmenares, O. Masek, W. Lisowski, D. Lisovytskiy, J. Grzonka and K. Kurzydlowski, *ChemCatChem*, 2018, **10**, 3469–3480.

125 H. Y. Fu, Z. C. Zhou, S. R. Zheng, Z. Y. Xu, P. J. J. Alvarez, D. Q. Yin, X. L. Qu and D. Q. Zhu, *Environ. Sci. Technol.*, 2018, **52**, 10453–10461.

126 M. J. Shi, W. Wei, Z. F. Jiang, H. K. Han, J. R. Gao and J. M. Xie, *RSC Adv.*, 2016, **6**, 25255–25266.

127 Z. Y. Jiang, X. H. Zhang, Z. M. Yuan, J. C. Chen, B. B. Huang, D. D. Dionysiou and G. H. Yang, *Chem. Eng. J.*, 2018, **348**, 592–598.

128 Y. L. Zhong, L. Hang, X. Q. Yin, H. F. Li, D. Fang and G. Hong, *ACS Sustainable Chem. Eng.*, 2018, **6**, 10660–10667.

129 C. J. Chen, Y. J. Li, J. W. Song, Z. Yang, Y. Kuang, E. Hitz, C. Jia, A. Gong, F. Jiang, J. Y. Zhu, B. Yang, J. Xie and L. B. Hu, *Adv. Mater.*, 2017, **29**, 8.